ISSN : 0974 - 7494 Volume 8 Issue 7

Nano Science and Nano Technology

An Indian Journal

Full Paper

NSNTAIJ, 8(7), 2014 [284-290]

Preparation and electromagnetic wave absorption hard- soft ferrite/polypyrrole core-shell nanocomposites

Seyed Hossein Hosseini[1]*, Ahmed Asadnia[2], Maryam Moloudi[3]
[1]Department of Chemistry, Faculty of Science, Islamshahr Branch, Islamic Azad University, Tehran, (IRAN)
[2]Young Researchers Club, Islamic Azad University, Center Tehran Branch, Tehran, (IRAN)
[3]Department of Chemistry, Faculty of Technical and Engineering, Saveh Branch, Islamic Azad University, Saveh, (IRAN)
E-mail : shhosseini@iiau.ac.ir

ABSTRACT

The nanocomposite of hard ($BaFe_{12}O_{19}$)/soft ferrite was prepared, and then the polypyrrole (PPy)-$BaFe_{12}O_{19}$/ Fe_3O_4 multi core–shell was produced by in situ polymerization method. X-ray diffraction, transmission electron microscope, scanning electron Microscopy and fourier transform infrared spectroscopy analysis indicated that Fe_3O_4 coated on the $BaFe_{12}O_{19}$ ferrite were homogenously enwrapped by PPy coating. The magnetic properties and electrical conductivity of the nanocomposite were characterized by vibrating sample magnetometer and four wire technique, respectively. As prepared conducting ferromagnetic polymer nanocomposites have electrical conductivity of the order of 5 S/cm and saturation magnetization (Ms) value of 3 emu/g. Microwave absorbing properties of the nanocomposite were investigated by using vector network analyzers in the frequency range of 8–12GHz. The values of the minimum reflection loss were -23 dB at 10 and -28 dB at 11.5 GHz for Fe_3O_4 coated on the $BaFe_{12}O_{19}$/ Fe_3O_4/PPy core/ shell nanocomposite with a thickness of 1.5 mm.

KEYWORDS

Composites;
Magnetic materials;
Chemical synthesis;
Magnetic properties;
Electrical properties.

INTRODUCTION

There has been a growing and widespread interest in microwave absorption materials for many years as a result of the serious electromagnetic interference pollution arising from mobile phones, radar systems and various electronic devices[1,2]. It is well known that the reflection and attenuation characteristic of EM-wave absorber is associated with complex permeability ($\mu=\mu'-j\mu''$), permittivity ($\varepsilon=\varepsilon'-j\varepsilon''$), EM impedance match, layer thickness and so on Magnetite as a conventional microwave absorption material has drawn considerable attention because of its high specific resistance and excellent microwave absorption property. However, magnetite has some difficulties based on increasing the permeability in GHz region because of Snoek limit induced by the electromagnetic wave[3]. Conducting polymer based composites with both electrical and magnetic properties have received tremendous attention in various fields such as electromagnetic interference (EMI) shielding, rechargeable batteries, corrosion equipment, and microwave absorbing materials etc[4-6].

Among various conducting polymers, PPy has been regarded as a new class of materials in the last few years due to their high electrical conductivity, easy preparation, and excellent environment stability[7,8]. To improve the electromagnetic properties and thus enlarge the application of the conducting polymers, the magnetic fillers such as ferrites are always added into the system. The nanocomposite ferrites consisting of the soft spinel ferrite and the hard M-type ferrite are promising due to their high remanence, high energy products, a low cost and an excellent corrosion resistance[9]. In addition, there are also some other core/shell nanostructures such as $ZnFe_2O_4$/polypyrrole, $Ni_{0.5}Zn_{0.5}Fe_2O_4$/bamboo charcoal Co/graphite, $BaFe_{12}O_{19}/TiO_2$, (Fe,Ni)/C nanocapsules and $La_{0.6}Sr_{0.4}MnO_3$ nanoparticles with amorphous shells have been studied for their improved microwave absorption properties[10-12]. The aim of the present study was the synthesis and the characterization of microwave absorbers. Thus, epoxy resin composites prepared with Fe_3O_4 coated on the $BaFe_{12}O_{19}$/PPy. The structure and the morphology of the samples were investigated by XRD and SEM. We also reported the microwave absorption property of such Fe_3O_4 coated on the $BaFe_{12}O_{19}$/PPy nanocomposite in the frequency range of 8–12 GHz. The attention has been paid on the structural development of polypyrrole nanocomposites, having dielectric and magnetic losses by the incorporation of Fe_3O_4 coated on the $BaFe_{12}O_{19}$ nanoparticles in the polypyrrole matrix.

EXPERIMENTAL SECTION

Materials

Pyrrole monomer (analytical grade, Merck) was distilled twice under reduced pressure and stored below 0 °C. Ferric chloride ($FeCl_3 . 6H_2O$), barium chloride dehydrate ($BaCl_2.2H_2O$), sodium hydroxide (NaOH), ammonium hydroxide, oleic acid, are analytical grades (Merck) and were used without further purification. DBSA and acrylic resin were of industrial grades.

Preparation of nanoparticles

(A) Barium ferrite ($BaFe_{12}O_{19}$)

Stoichiometric amounts of barium chloride, was dissolved completely into ultra pure water to make an aqueous solution (I). Ferric chloride was separately mixed in ultra pure water to make another aqueous solution (II). Both the above solutions were mixed in a 1:1 molar ratio. The brownish colored ferrite particles were precipitated from this mixture by gradually adding sodium hydroxide, NaOH (7.5 M) solution at room temperature (pH=12). The aqueous suspension was stirred gently for 15 min to achieve chemical homogeneity. The precipitates so formed were filtered off, washed with water and dried at 100 °C overnight. The precipitated nanocrystalline powder was mixed thoroughly with NaCl in 1:2 ratios (W:W). Since the melting point of NaCl is about 800 °C, so the 'as synthesized' particles were given a heat treatment 1200 °C for 4 h in nitrogen atmosphere to achieve a uniform growth. During annealing, there was liquid phase diffusion of particles surrounding the molten NaCl salt which makes the process fast and hexaferrite particles crystallize out completely with uniform morphology after cooling in the furnace. The cooled mixture of nanoparticles and NaCl was then washed by ultra pure water. NaCl was dissolved and $BaFe_{12}O_{19}$ nanoparticles were filtered out.

(B) Iron ferrite (Fe_3O_4)

$FeCl_3.6H_2O$ (24.3 g) and $FeSO_4.7H_2O$ (16.7 g) were dissolved in 100 mL de-ionized water under nitrogen gas with vigorous stirring at 80 °C. Then 50 ml of ammonium hydroxide were added rapidly into the solution. The color of the solution turned to black immediately. Oleic acid (3.76 g) was added after 30 min. Then the suspension was kept at 80 °C for 1.5 h. The magnetite nanoparticles were washed with de-ionized water until the pH value of the system reached neutral. The synthesized sample was dried in vacuum at room temperature.

Preparation of Fe_3O_4 - coated on the $BaFe_{12}O_{19}$ ($BaFe_{12}O_{19}/Fe_3O_4$)

0.1 g nano-sized particles of prepared $BaFe_{12}O_{19}$ were dispersed in 200 ml water solution of pH 6 under ultra soniûcation for 2 min. At this pH, the surface charge of $BaFe_{12}O_{19}$ in the solution is expected to bepositive, and that of Fe_3O_4 to be negative. The two solutions were mixed at 1/19 volumetric ratio (1/19 weight ratio of $BaFe_{12}O_{19}/ Fe_3O_4$) and subjected to soniûcation for 2 min so that $BaFe_{12}O_{19}$ particle was coated with Fe_3O_4 particles. The solution was then ûltered using ultraûltration membrane and dried at room temperature. We also prepared physically mixed Fe_3O_4 and $BaFe_{12}O_{19}$ by mixing the two solid Fe_3O_4 and $BaFe_{12}O_{19}$ samples with 1/19 weight ratio of $BaFe_{12}O_{19}/Fe_3O_4$ for 1 h using a rotating machine.

Synthesis of hard- soft ferrite/PPy nanocomposites with multi core–shell structure

$BaFe_{12}O_{19}/Fe_3O_4$/PPy, multi core–shell and Fe_3O_4/PPy, $BaFe_{12}O_{19}$/PPy core–shell nanocomposites were prepared by in situ polymerization in the presence of DBSA as the surfactant and $FeCl_3$ as the oxidant, were also prepared by in situ polymerization. The DBSA in distilled water was dissolved in distilled water by vigorous stirring for 20 min, then nanoparticles (0.73 g) under stirring for approximately 1 h were added to the DBSA solution. 5 mL of pyrrole monomer was added to the suspension and stirred for 30 min. nanoparticles, in the mixture of pyrrole/DBSA under ultra sonicaction, were dispersed well in 2 h. 23.5 g $FeCl_3$ was added slowly in 60 mL deionized water dropwise to the mixture with a constant stirring. Then under an ice-water bath the polymerization was allowed to proceed in 4 h. Final nanocomposite was obtained by filtering and washing with deionized water and ethanol, respectively. The obtained black powder with a content of 15 wt% nanoparticles was dried in 24 h under vacuum.

Characterization

The morphology of coated particles and nanocomposite was observed SEM with a JSM-6301F (Japan) instrument operated at an accelerating voltage of 10 kV. XRD patterns of the nanoparticles assembles were collected on a Philips-PW 1800 with Cu-K radiation under Cu Kα radiation (λ=1.5406 Å). The size and morphology of the as-synthesized products were characterized by a JEM-200CX TEM at 160 kV. Fourier transform infrared spectroscopy (FTIR) spectra were recorded on a PerkinElmer spectrum FTIR using KBr pellets. The magnetic properties (intrinsic coercivity, saturation, the M–H hysteresis loops and remanent magnetization) were recorded by using a vibrating sample magnetometer (VSM, MDK6), which has been made by the efforts of the Magnetis Daghigh Kavir Company in Iran. The conductivity of the composite was measured by four point probe method using a SX1944 four-point probe instrument (Baishen Science Co. China). Microwave absorbing properties were measured by a HP 8720B vector network analyzer and standard horn antennas in anechoic chamber.

RESULTS AND DISCUSSION

X-ray diffraction

The XRD pattern of Fe_3O_4, $BaFe_{12}O_{19}$ and $BaFe_{12}O_{19}/Fe_3O_4$ have been showed in Figure 1. It should be noticed, that there were some peaks of α-Fe_2O_3 in the XRD pattern of Fe_3O_4 (2θ=33,54) and $BaFe_{12}O_{19}$ (2θ=54) nanoparticles. All peaks correspond to the characteristic peaks of cubic type lattice of $BaFe_{12}O_{19}$ (JCPDS file no. 88-1965) and Fe_3O_4 (JCPDS file no. 19-0629). From the obtained peak width of XRD patterns, the sizes of $BaFe_{12}O_{19}$, Fe_3O_4 and $BaFe_{12}O_{19}/Fe_3O_4$ nanoparticles were calculated 24.27, 7.38 and 31.65 nm, respectively using the Debye–Scherrer equation. The XRD pattern indicated that $BaFe_{12}O_{19}/Fe_3O_4$ nanocomposites have been formed. Compared to $BaFe_{12}O_{19}$ and Fe_3O_4 nanoparticles, the intensity of the characteristic peaks of α-Fe_2O_3 decreased in the $BaFe_{12}O_{19}/Fe_3O_4$ nanocomposites. This may be attributed to the coating of Fe_3O_4 nanoparticles on the surface of $BaFe_{12}O_{19}$ nanoparticles.

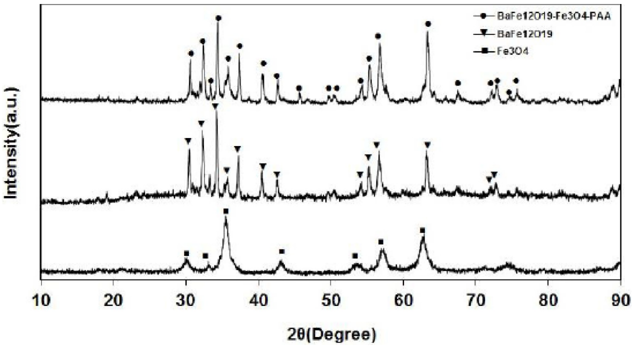

Figure 1 : X-ray diffraction pattern for Fe_3O_4, $BaFe_{12}O_{19}$ and $BaFe_{12}O_{19}/Fe_3O_4$ nanoparticles

FTIR spectra

The FTIR spectra of PPy, $BaFe_{12}O_{19}/Fe_3O_4$ and $BaFe_{12}O_{19}/Fe_3O_4$/PPy nanocomposite, have been showed in Figure 2(a-c). The characterized peaks of PPy was occured at 3200-3500, 1627, 1541, 1447, 1309, 1198, 1189, 1089, 1038, 789 and 663 cm^{-1} (Figure 2a). The peak at 3200-3500 cm^{-1} was attributed to the characteristic N-H vibration stretching of PPy. The peaks at 1627, 1541 and 1447 cm^{-1} were attributed to the characteristic C=C, C=N and C-N stretching of the quinoid and benzenoid rings of PPy. The peaks at 1309 and 1198 cm^{-1} corresponded to N–H bending and asymmetric C–N stretching modes of the benzenoid ring, respectively. The peak around 1189 cm^{-1} was associated with vibrational modes of N=Q=N (Q refers to the quinonic type rings) which indicated that PPy was formed in our sample. In ferrites, according to the geometrical configuration of the oxygen nearest neighbors the metal ions are usually situated in two different sub-lattices, which are designated as tetrahedral and octahedral sites. The peaks at 587 and 547 cm^{-1} were intrinsic vibrations of Fe-O in Fe_3O_4 and $BaFe_{12}O_{19}$ (Figure 2b).

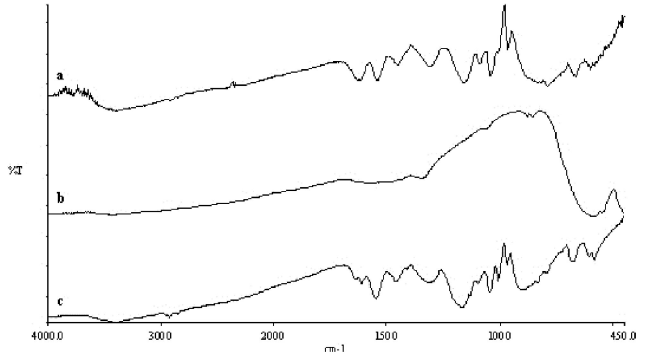

Figure 2 : FTIR spectra: (a) PPy (b) $BaFe_{12}O_{19}/Fe_3O_4$ nanoparticles and (c) $BaFe_{12}O_{19}/Fe_3O_4$/PPy nanocomposite

The characteristic peaks of $BaFe_{12}O_{19}/Fe_3O_4$/PPy nanocomposite were occured at 3200-3500, 2930, 1609, 1548, 1461, 1330, 1166, 1046, 1006, 888, 681, 591 and 587 cm^{-1} (Figure 2c). The peak at 3200-3500 cm^{-1} was attributed to the characteristic N-H vibration stretching of PPy. The peaks at 1609, 1548 and 1461 cm^{-1} were attributed to the characteristic C=C, C=N and C-N stretching of the quinoid and benzenoid rings of PPy. The peaks at 1330 and 1166 cm^{-1} corresponded to N–H bending and asymmetric C–N stretching modes of the benzenoid ring, respectively.

The peaks at 2930 and 1028 cm^{-1} were attributed to the symmetric and anti-symmetric stretching vibration of C-H and SO_3 group of dopant (DBSA). The peaks at1006 and 888 cm^{-1} were attributed to the p-disubstituted aromatic ring C–H out-of-plane bending. However, the characteristic peaks of Fe_3O_4 and $BaFe_{12}O_{19}$ could be observed only at higher wavenumbers (591 and 587 cm^{-1}) which indicated that there was an interaction between $BaFe_{12}O_{19}/Fe_3O_4$ nanoparticles and PPy chain.

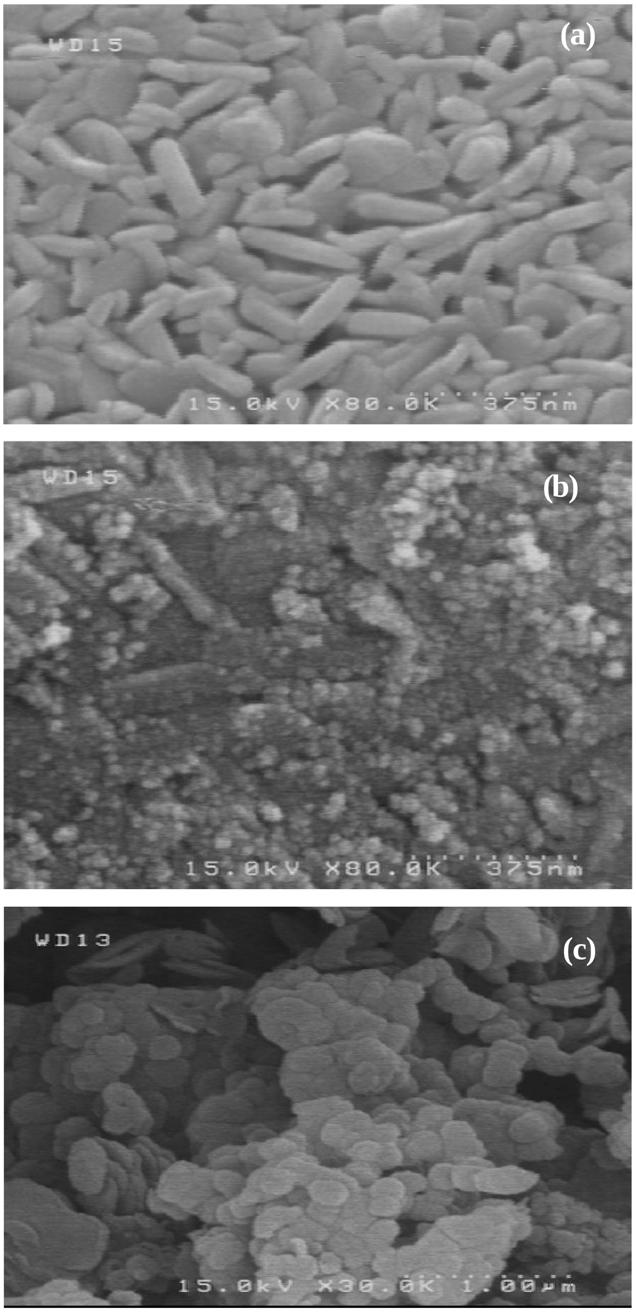

Figure 3 : FE-SEM images of (a) $BaFe_{12}O_{19}$, (b) $BaFe_{12}O_{19}/Fe_3O_4$ and (c) $BaFe_{12}O_{19}/Fe_3O_4$/PPy

Morphology investigation

Figure 3(a-c) shows the SEM images for a) $BaFe_{12}O_{19}$, b) $BaFe_{12}O_{19}/Fe_3O_4$ nanoparticles and c) $BaFe_{12}O_{19}/Fe_3O_4$/*PPy* nanocomposite, respectively. As shown in Figure 3(a), the rod-shaped $BaFe_{12}O_{19}$ was seen in a small quantity of amorphous phase. Average diameter of rod-shape was in the range of 30-40 nm. Figure 3(b) shows the SEM image for core-shell $BaFe_{12}O_{19}/Fe_3O_4$ nanoparticles. Average diameters were in the range of 15-20 nm for Fe_3O_4 and 40-50 nm for $BaFe_{12}O_{19}/Fe_3O_4$. In Figure 3(c), it is found that the $BaFe_{12}O_{19}/Fe_3O_4$/PPy nanocomposite (15 wt%) still retained the morphology of PPy flake-shape. It is not clear how rod-shaped composite was formed in the polymerization process. Average diameter was in the range of 70-120 nm for $BaFe_{12}O_{19}/Fe_3O_4$/PPy nanocomposite.

TEM analysis

Average particle size of the $BaFe_{12}O_{19}/Fe_3O_4$ nanoparticles measured using TEM analysis and micrographs for the powder were in Figure 4. The photographs indicated that average particle sizes of the powders were in the 35–45 nm range. Particles were uniformly elongated and formed loose aggregates.

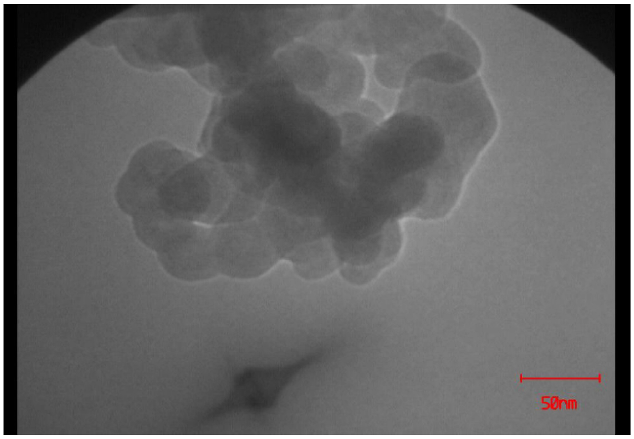

Figure 4 : TEM micrographs for $BaFe_{12}O_{19}/Fe_3O_4$ nanocomposites

Magnetic properties

Magnetic properties of the samples were measured with a VSM at room temperature. The hysteresis loops are illustrated in Figure 5(a,b). This Figure shows the magnetization (M) versus the applied magnetic field (H) for a) Fe_3O_4, $BaFe_{12}O_{19}/Fe_3O_4$ nanoparticles and b) $BaFe_{12}O_{19}/Fe_3O_4$/PPy nanocomposite (15 wt%), respectively. It could be inferred from the hysteresis loops that all composite magnetic spheres were soft magnetically at room temperature with an applied field $-10\ \text{kOe} \le H \le 10\ \text{kOe}$. TABLE 1 shows all values saturation magnetization (M_s), remnant magnetization (M_r) and coercivity field (Hc) for Fe_3O_4, $BaFe_{12}O_{19}/Fe_3O_4$ nanoparticles and $BaFe_{12}O_{19}/Fe_3O_4$/PPy nanocomposite (15 wt%).

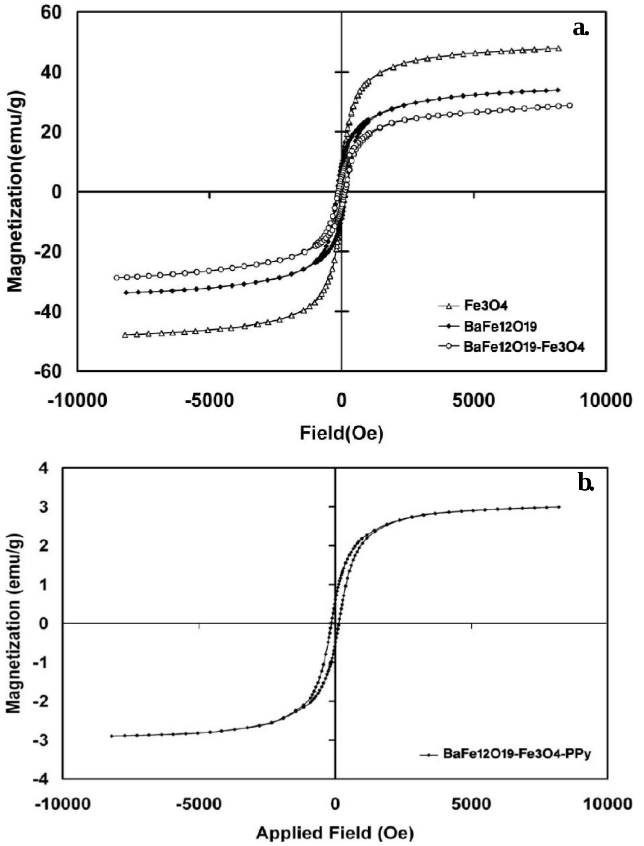

Figure 5 : The hysteresis loops a) Fe_3O_4, $BaFe_{12}O_{19}$, $BaFe_{12}O_{19}/Fe_3O_4$ nanoparticles and b) $BaFe_{12}O_{19}/Fe_3O_4$/PPy nanocomposite (15 wt%)

Figure 5 shows M_s and M_r Fe_3O_4 is higher than $BaFe_{12}O_{19}$, $BaFe_{12}O_{19}/Fe_3O_4$ and $BaFe_{12}O_{19}/Fe_3O_4$/PPy, but H_c is lower. In the other hands, $BaFe_{12}O_{19}/Fe_3O_4$/PPy nanocomposite is lower than pure and core-shell nanoparticles. The electrical conductivity of PPy was decrease magnetic property. Magnetic properties of nanocomposites containing magnetite or ferrite particles have been believed to be highly dependent on the sample shape, crystallity, and the value of magnetic particles. Therefore, they could be adjusted to obtain optimum magnetic property. Although the $BaFe_{12}O_{19}/Fe_3O_4$ nanocomposites consisted of two magnetic phases, the hysteresis loop showed a single-phase-like behavior, and the magnetization changed with the applied field smoothly. This indicated that the $BaFe_{12}O_{19}$ core and Fe_3O_4 first shell contact intimately. The values of saturation magnetization Ms decreased from 47.8 and 33.9 emu/g for pure Fe_3O_4 and $BaFe_{12}O_{19}$ to 28.7 emu/g for the core-shell structure nanocomposites owing to the coating of Fe_3O_4.

The change of the saturation magnetization and the coercivity could be attributed to the existence of Fe_3O_4 on the surface of $BaFe_{12}O_{19}$ nanoparticles, which resulted in the interparticle interaction at the interface of two phases. Based on saturation magnetization, the interphase interaction leaded to the non-collinearity of the magnetic moments at the interface of two phases. So, saturation magnetization was reduced. For coercivity, when the particles contact closely, coupling interphase exchange occurs. So, the rotation of the domains on one particle as the field was reversed, induces domains in contiguous particles to rotate, and thereby decreased the coercivity.

TABLW 1 : The values of saturation magnetization (M_s), remnant magnetization (M_r) and coercivity field (Hc) for Fe_3O_4, $BaFe_{12}O_{19}/Fe_3O_4$ nanoparticles and $BaFe_{12}O_{19}/Fe_3O_4$/PPy nanocomposite (15 wt%)

Sample	Saturation Magnetization (M_s) (emu/g)	Remnant Magnetization (M_r) (emu/g)	Coercivity Field (Hc)(Oe)
Fe_3O_4	47.8	15	0
$BaFe_{12}O_{19}$	33.9	13	181
$BaFe_{12}O_{19}/Fe_3O_4$	28.7	8	125
$BaFe_{12}O_{19}/Fe_3O_4$/PPy	3	0.8	120

Conductivity

Electrically conductivity of samples at room temperature was measured by four probe method. When the PPy was doped by DBSA, the conductivity was improved from 10 to 45 S/cm, suggesting that doping H^+ increased conductivity of PPy. When 15% of mass content of $BaFe_{12}O_{19}/Fe_3O_4$ nanoparticles was incorporated, the conductivity of $BaFe_{12}O_{19}/Fe_3O_4$/PPy nanocomposite was sharply reduced from 45 to 5 S/cm. The decrease in conductivity of $BaFe_{12}O_{19}/Fe_3O_4$/PPy composites, by $BaFe_{12}O_{19}/Fe_3O_4$ in the core of the nanoparticles may be attributed to the insulting behavior of the ferrite and partial blockage of the conductive path.

Electromagnetic waves absorbing properties

In order to investigate the electromagnetic waves absorbing properties of the resulting products, the variation of reflection loss, RL (dB), versus frequency in the range of 8-12 GHz was illustrated. Generally, the RL of an absorber can be concluded from the equation (1):

$$RL = 20\log\left|\frac{Z_{in}-Z_0}{Z_{in}+Z_0}\right| \qquad (1)$$

Where Z_0 is the characteristic impedance of free space, Z_{in} is the normalized input impedance at free space and materials interface, which is determined by the following relation:

$$Z_{in} = (\mu_r/\varepsilon_r)^{1/2}\tanh[(j2\pi ft/c)(\mu_r\varepsilon_r)^{1/2}] \qquad (2)$$

Where ε_r and μ_r are the complex permittivity and the complex permeability of the prepared samples, respectively. *C* is the velocity of electromagnetic waves in free space, *f* is the frequency of the microwave and *t* is the thickness of prepared absorber[9]. The reflection-loss peak in the case of samples with the spinel structure (Fe_3O_4/PPy) shifted to a lower frequency along with the increased thickness and the peak value became bigger and narrower. This showed that by changing the thickness of the material with the spinel structure the position and the attenuation-peak frequency could be easily manipulated in terms of the frequency range. In contrast, the reflection loss for samples with the hexagonal structure ($BaFe_{12}O_{19}$/PPy) was found to depend sensitively on the absorber thickness in the frequency range from 400 MHz to 32 GHz. These results were in a good agreement with the phenomenon that a decrease in the coercivity may be responsible for the magnetic resonance reduction and as a consequence the thinning of the peaks of the reflection loss[12]. We can conclude that composite materials with a larger fraction of the spinel phase/structure can be used as electromagnetic wave absorbers in the lower GHz range, while composite materials with a larger fraction of hexagonal phase might be used in the GHz range above 32 GHz, due to their dielectric and magnetic losses. However, there is a range of compositions that can cover a broad range of frequency absorption, which was the aim of this contribution.

Nanocomposites powders were dispersed in *PPy* then the mixture was pasted on metal plate with the area of 40mm×40mm as the test plate. The microwave absorbing properties of the nanocomposite with the coating thickness of 1 mm were investigated by using a HP 8720B vector network analyzer and standard horn antennas in anechoic chamber in the frequency range of 8–12 GHz. The microwave absorption behaviors of the PPy, Fe_3O_4/PPy, $BaFe_{12}O_{19}$/PPy and $BaFe_{12}O_{19}$/

Fe_3O_4/PPy nanocomposites were showed in Figure 6 with the coating thickness of 1 mm. For Fe_3O_4/PPy and $BaFe_{12}O_{19}$/PPy nanocomposites the minimum reflection losses were -11, -13, -18 and -13 dB at the frequency of 8.7, 9.5, 10.4 and 11.5 GHz, respectively. For $BaFe_{12}O_{19}$/PPy nanocomposites the minimum reflection losses were -12, -18, -20 and -25 dB at the frequency of 8.5, 9.6, 10.5 and 11.5 GHz, respectively. For $BaFe_{12}O_{19}/Fe_3O_4$/PPy multi core–shell nanocomposite the reflection loss values of minimum reflection losses were -10, -23 and -28 dB at the frequencies of 8.8, 10.0 and 11.7 GHz, respectively. For $BaFe_{12}O_{19}/Fe_3O_4$/PPy multi core–shell nanocomposite the reflection loss values of less than -28 dB were obtained in the frequency of 8–12 GHz. The absorption values in $BaFe_{12}O_{19}$/PPy and $BaFe_{12}O_{19}/Fe_3O_4$/PPy multi core–shell nanocomposite are increased by increasing rod-shape particles (Ba) and electrical conductivity property (PPy).

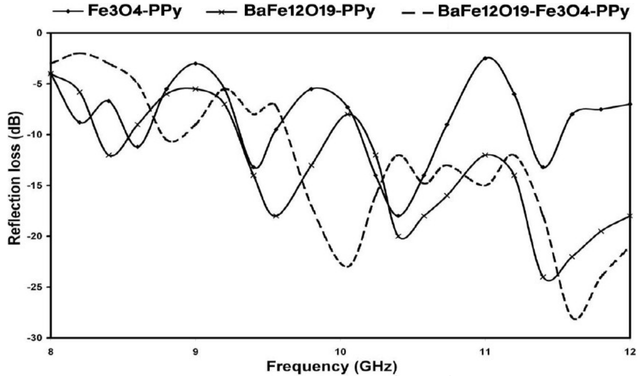

Figure 6 : Frequency dependence of RL for the Fe_3O_4/PPy, $BaFe_{12}O_{19}$/PPy and $BaFe_{12}O_{19}/Fe_3O_4$/PPy

CONCLUSION

The ferrite polymer nanocomposites with different ferrites have been successfully prepared in PPy matrix. $BaFe_{12}O_{19}/Fe_3O_4$/PPy multi core–shell nanocomposite with the magnetic and electrical behaviors was synthesized successfully by in situ polymerization of pyrrole in the presence of $BaFe_{12}O_{19}/Fe_3O_4$ nanoparticles. The microwave absorption properties of $BaFe_{12}O_{19}/Fe_3O_4$/PPy multi core–shell nanocomposite were better than of Fe_3O_4/PPy and $BaFe_{12}O_{19}$/PPy nanocomposites. That is for rod-shape particles and conductivity properties. For $BaFe_{12}O_{19}/Fe_3O_4$/PPy multi core–shell nanocomposite with the coating thickness of 1 mm the reflection losses values less than -28 dB were obtained in the frequency of X-band. The introduction of PPy improved the absorbing properties, which was due to the dielectric loss of PPy. Such strong absorption is attributed to better electromagnetic matching due to the existence of PPy and the special core/shell structure. Therefore, the prepared composites have potential applications in EMI shielding.

REFERENCES

[1] G.Tong, W.Wu, J.Guan, H.Qian, J.Yuan, W.Li; Journal of Alloys and Compounds, **509**, 4320 **(2011)**.

[2] Z.He, Y.Fang, X.Wang, H.Pang; Synthetic Metals, **161**, 420 **(2011)**.

[3] Y.Li, G.Chen, Q.Li, G.Qiu, X.Liu; Journal of Alloys and Compounds, **509**, 4104 **(2011)**.

[4] J.C.Aphesteguy, A.Damiani, D.D.Giovanni, S.E.Jacobo; Physica B, **407**, 3168 **(2012)**.

[5] G.V.Kurlyandskaya, J.Cunanan, S.M.Bhagat, J.C.Aphesteguy, S.E.Jacobo; Journal of Physics and Chemistry of Solids, **68**, 1527 **(2007)**.

[6] J.C.Aphesteguy, P.G.Bercoff, S.E.Jacobo; Physica B, **398**, 200 **(2007)**.

[7] S.H.Hosseini, S.H.Mohseni, A.Asadnia, H.Kerdari; Journal of Alloys and Compounds, **509**, 4682 **(2011)**.

[8] H.Pang, M.Fan, Z.He; Journal of Magnetism and Magnetic Materials, **324**, 2492 **(2012)**.

[9] S.H.Hosseini, A.Asadnia; Journal of Nanomaterials, **2012**, 1687 **(2012)**.

[10] J.Qiu, Y.Wang, M.Gu; J.Mater.Sci., **42**, 166 **(2007)**.

[11] Z.Xiey, D.Geng, X.Liu, S.Ma, Z.Zhang; J.Mater.Sci.Technol., **27(7)**, 607 **(2011)**.

[12] A.Drmota, J.Koselj, M.Drofenik, A.Znidarsic; Journal of Magnetism and Magnetic Materials, **324**, 1225 **(2012)**.